

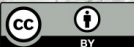
Tectonics from topography

Insights from high-resolution hillslope morphology analysis



GM2.1

EGU2020-2985



Godard V.¹, Hippolyte J.-C.¹, Cushing E.², Espurt N.¹

Fleury J.¹, Bellier O.¹, Ollivier V.³ & ASTER Team¹

¹CEREGE, Aix-Marseille Université, Aix-en-Provence, France

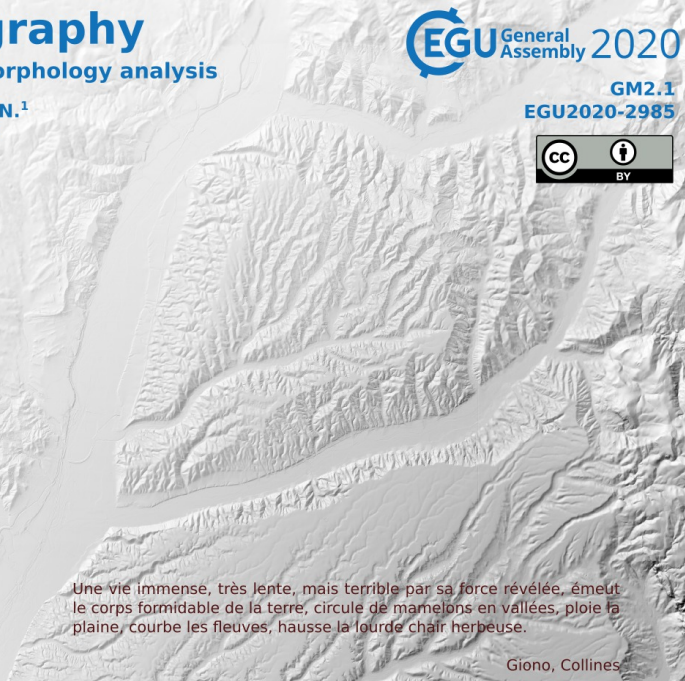
²BERSSIN, IRSN, Fontenay-aux-Roses, France

³LAMPEA, Aix-Marseille Université, Aix-en-Provence, France



IRSN

INSTITUT
DE RADIOPROTECTION
ET DE SÛRETÉ NUCLÉAIRE



Une vie immense, très lente, mais terrible par sa force révélée, émeut le corps formidable de la terre, circule de mameions en vallées, ploie la plaine, courbe les fleuves, hausse la lourde chair herbeuse.

Giono, Collines

Also at...

<https://doi.org/10.5194/esurf-8-221-2020>



Earth Surface Dynamics
An interactive open-access journal of the European Geosciences Union

| EGU.eu | EGU Publications | EGU Highlight Articles | Contact | Imprint | Data protection |

Articles

Earth Surf. Dynam., 8, 221–243, 2020
<https://doi.org/10.5194/esurf-8-221-2020> 

© Author(s) 2020. This work is distributed under the Creative Commons Attribution 4.0 License.


Research article

Hillslope denudation and morphologic response to a rock uplift gradient

Vincent Godard^{1,2}, **Jean-Claude Hippolyte**^{2,3}, **Edward Cushing**^{2,4}, **Nicolas Espurt**², **Jules Fleury**², **Olivier Bellier**², **Vincent Ollivier**^{2,5}, and the ASTER Team⁶

¹Aix-Marseille Univ., CNRS, IRD, INRAE, Coll France, CEREGE, Aix-en-Provence, France
²Institut Universitaire de France (IUF), Paris, France
³PSE-ENV/SCAN, Institut de Radioprotection et de Sûreté Nucléaire, Fontenay-aux-Roses, France
⁴Aix-Marseille Univ., CNRS, Ministry of Culture, LAMPEA, Aix-en-Provence, France
⁵A full list of authors appears at the end of the paper.

Correspondence: Vincent Godard (godard@cerege.fr)

Received: 17 Sep 2019 – Discussion started: 25 Oct 2019 – Revised: 16 Feb 2020 – Accepted: 03 Mar 2020 – Published: 07 Apr 2020

Abstract

Documenting the spatial variability of tectonic processes from topography is routinely undertaken through the analysis of river profiles, since a direct relationship between fluvial gradient and rock uplift has been identified by incision models. Similarly, theoretical formulations of hillslope profiles predict a strong dependence on their base-level lowering rate, which in most situations is set by channel incision. However, the reduced sensitivity of near-threshold hillslopes and the limited availability of high-resolution topographic data has often been a major limitation for their use to investigate tectonic gradients. Here we combined high-resolution analysis of hillslope morphology and cosmogenic-nuclide-derived denudation rates to unravel the distribution of rock uplift across a blind thrust system at the southwestern Alpine front in France. Our study is located in the Mio-Pliocene Valensole mioscopic basin, where a series of folds and thrusts has deformed a plateau surface. We focused on a series of catchments aligned perpendicular to the main structures. Using a 1 m lidar digital terrain model, we extracted hillslope topographic properties such as hilltop curvature C_{HT} and nondimensional erosion rates E^* . We observed systematic variation of these metrics coincident with the location of a major underlying thrust system identified by seismic surveys. Using a simple deformation model, the inversion of the E^* pattern allows us to propose a location and dip for a blind thrust, which are consistent with available geological and geophysical data. We also sampled clasts from eroding conglomerates at several hilltop locations for ^{10}Be and ^{26}Al concentration measurements. Calculated hilltop denudation rates range from 40 to 120 mm kyr⁻¹. These denudation rates appear to be correlated with E^* and C_{HT} that were extracted from the morphological analysis, and these rates are used to derive absolute estimates for the fault slip rate. This high-resolution hillslope analysis allows us to resolve short-wavelength variations in rock uplift that would not be possible to unravel using commonly used channel-profile-based methods. Our joint analysis of topography and geochronological data supports the interpretation of active thrusting at the southwestern Alpine front, and such approaches may bring crucial complementary constraints to morphotectonic analysis for the study of slowly slipping faults.

ESurf | Articles | Volume 8, Issue 2  **Copernicus Publications**
The Innovative Open Access Publisher

Search articles
Search
Author 

Download
 **PDF**  **FULL TEXT**  **XML**

Short summary
Slow-slipping faults are often difficult to identify in landscapes. Here we analyzed...


Read more

Citation
 **BibTeX**
 **EndNote**

Share
      

Similar articles

 **Drainage divide networks – Part 1...** Scherler et al.

 **Drainage divide networks – Part 2...** Scherler et al.

 **Geomorphic signatures of the transient ...** Beeson et al.

Tectonic from topography

Geological Society of America
Special Paper 398
2006

Tectonics from topography: Procedures, promise, and pitfalls

Cameron Wobus[†]
Kelin X. Whipple

*Department of Earth, Atmospheric and Planetary Sciences, Massachusetts Institute of Technology,
Cambridge, Massachusetts 02139, USA*

Eric Kirby

Department of Geosciences, The Pennsylvania State University, University Park, Pennsylvania 16802, USA

Noah Snyder

Department of Geology and Geophysics, Boston College, Chestnut Hill, Massachusetts 02467, USA

Joel Johnson

Katerina Spyropolou
Benjamin Crosby

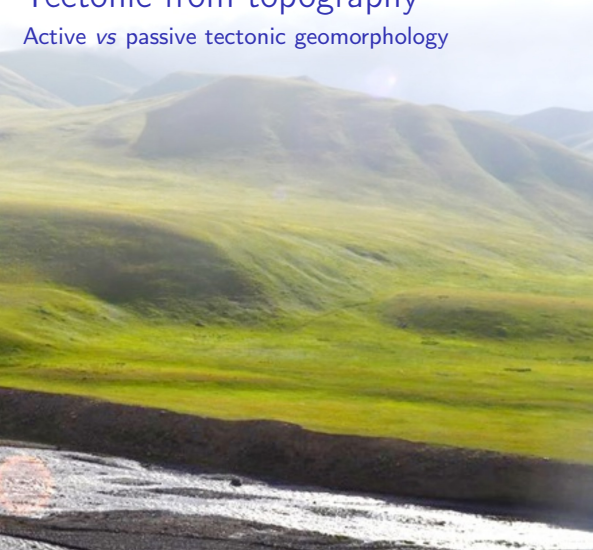
*Department of Earth, Atmospheric and Planetary Sciences, Massachusetts Institute of Technology,
Cambridge, Massachusetts 02139, USA*

Daniel Sheehan

Information Systems, Massachusetts Institute of Technology, Cambridge, Massachusetts 02139, USA

Tectonic from topography

Active vs passive tectonic geomorphology



Passively deformed landforms

Talas-Fergana Fault
Arpa Basin (Kyrgyzstan)
Magali Rizza

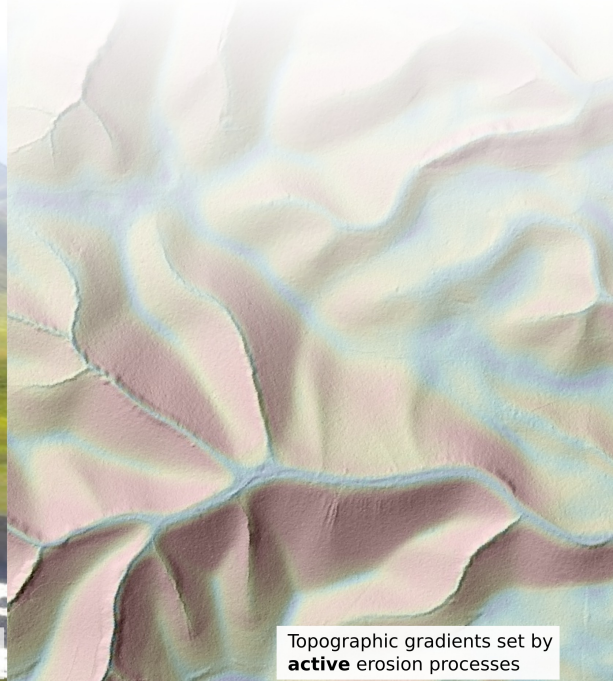
Tectonic from topography

Active vs passive tectonic geomorphology



Passively deformed landforms

Talas-Fergana Fault
Arpa Basin (Kyrgyzstan)
Magali Rizza



Topographic gradients set by
active erosion processes

Tectonics from fluvial and hillslope processes

River profile response

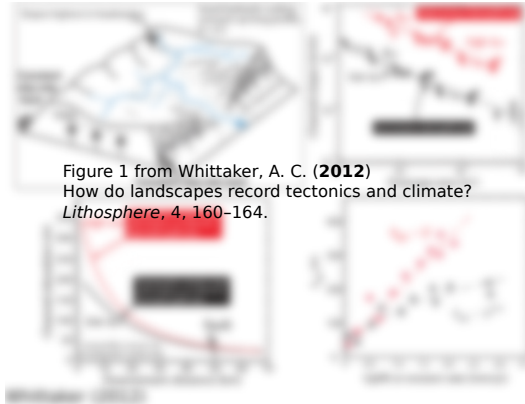


Figure 1 from Whittaker, A. C. (2012)
How do landscapes record tectonics and climate?
Lithosphere, 4, 160–164.

- ▶ Scales with uplift rate over large range
- ▶ Limitation from erodibility variations,
knickpoints, structure of river networks

Tectonics from fluvial and hillslope processes

River profile response

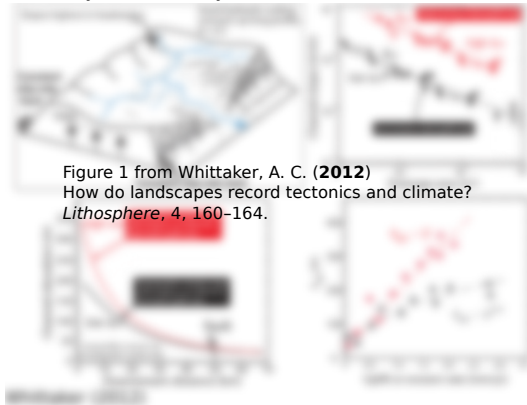


Figure 1 from Whittaker, A. C. (2012)
How do landscapes record tectonics and climate?
Lithosphere, 4, 160–164.

Hillslope gradient response

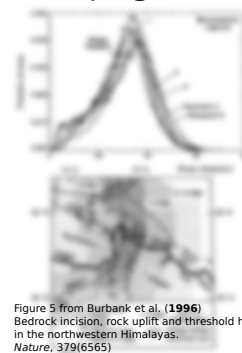


Figure 5 from Burbank et al. (1996)
Bedrock incision, rock uplift and threshold hillslopes
in the northwestern Himalayas.
Nature, 379(6565)

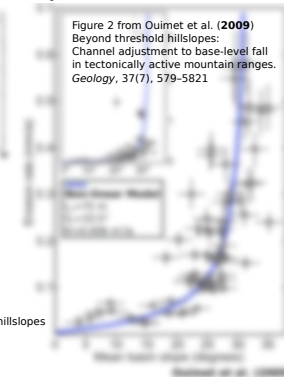


Figure 2 from Ouimet et al. (2009)
Beyond threshold hillslopes:
Channel adjustment to base-level fall
in tectonically active mountain ranges.
Geology, 37(7), 579–582

- ▶ Scales with uplift rate over large range
- ▶ Limitation from erodibility variations, knickpoints, structure of river networks

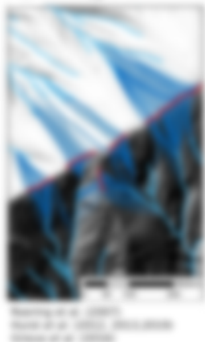
- ▶ Potentially very high spatial density of information
- ▶ But hillslope gradient response limited by threshold angle S_c

Hillslope processes and response

Insights from High-Resolution topographic analysis

Hillslope topographic profile

Figure 6 from Hurst et al. (2012)
Using hilltop curvature to derive
the spatial distribution of erosion rates
Journal of Geophysical Research,
117(F2), F02017



$$z(x) = \frac{KS_c^2}{2\beta E} \left(\ln \left(\frac{1}{2} \sqrt{1 + \left(\frac{2\beta Ex}{KS_c} \right)^2} + \frac{1}{2} \right) - \sqrt{1 + \left(\frac{2\beta Ex}{KS_c} \right)^2} + 1 \right)$$

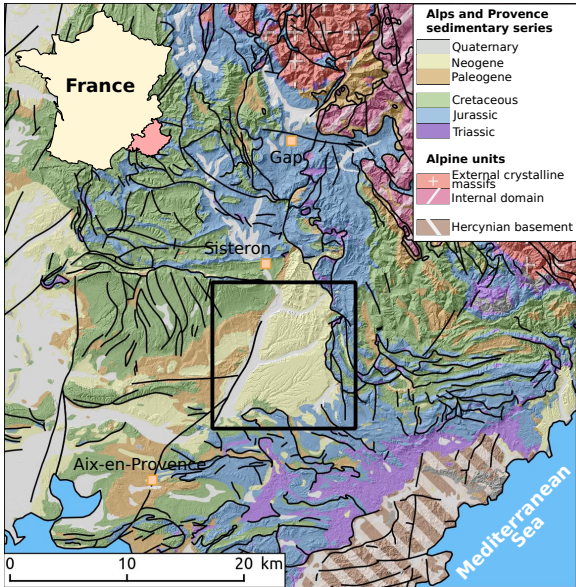
Non-dimensional form

$$R^* = \frac{R}{S_c L_H} \quad E^* = \frac{2C_{HT} L_H}{S_c}$$

$$R^* = \frac{1}{E^*} \left(\sqrt{1 + (E^*)^2} - \ln \left(\frac{1}{2} \left(1 + \sqrt{1 + (E^*)^2} \right) \right) - 1 \right).$$

- ▶ Hilltop curvature $C_{HT} \Rightarrow$ proxy for erosion rate : $E = \frac{KC_{HT}}{\beta}$
- ▶ Possibility to retrieve tectonic information from hillslope morphology
- ▶ Limited number of case studies so far

Settings



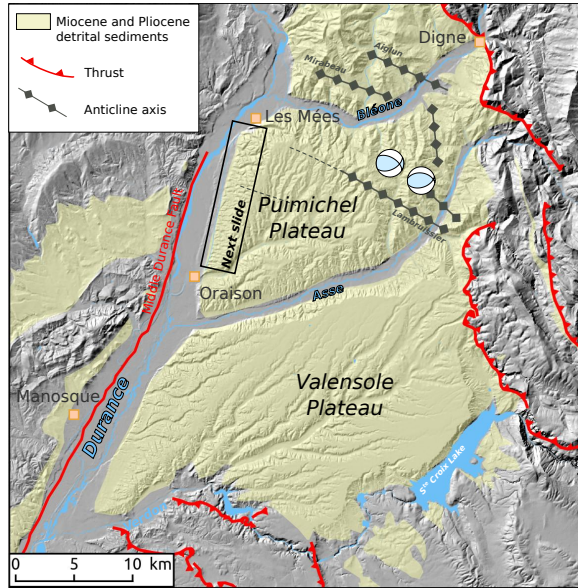
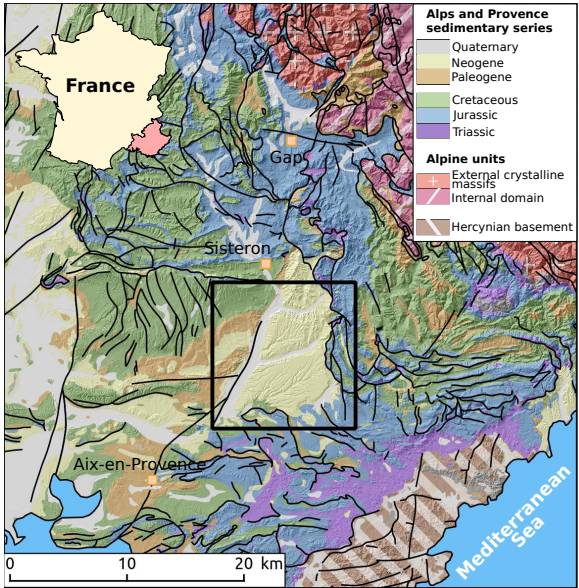
Provence and SW Alps

- ▶ Slow deformation
- ▶ Significant seismic hazard
- ▶ e.g. 1909 Lambesc Earthquake



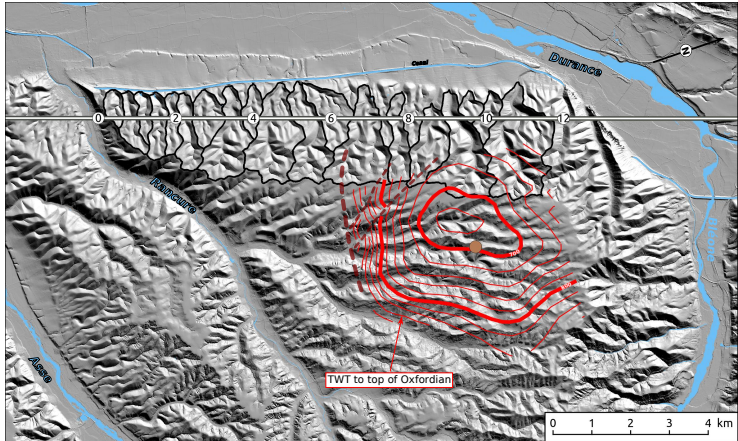
Specific challenges for the identification of slow faults under temperate climate

Settings



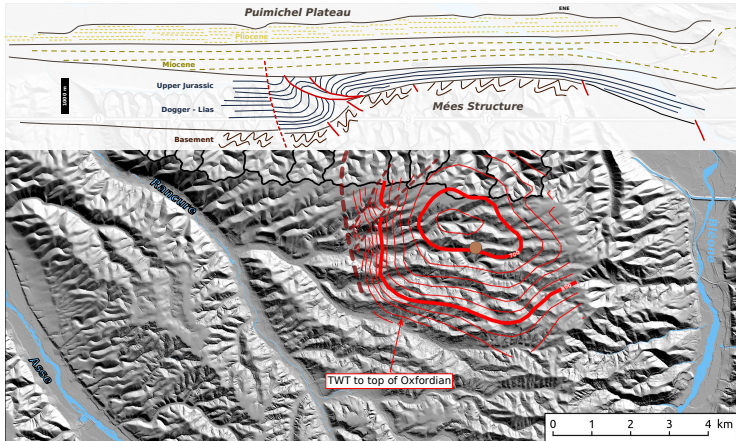
Settings

- ▶ Puimichel Plateau
 - Uplifted Mio-Pliocene molassic deposits
 - Major depocenter of the SW Alps
- ▶ Mées structure
 - Csup-Eocene basement deformation (Pyrenean orogeny)
 - Possible Alpine reactivation



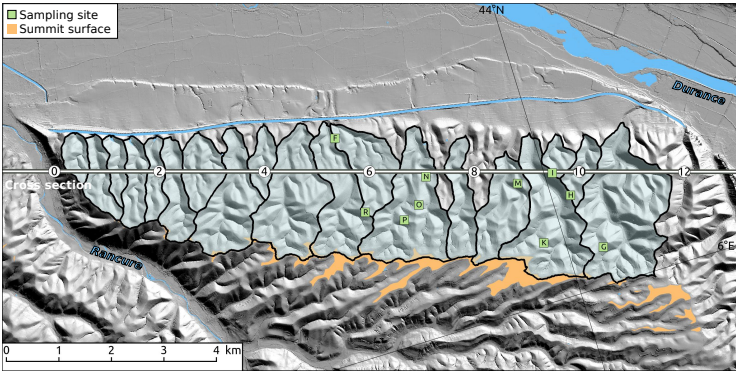
Settings

- ▶ Puimichel Plateau
 - Uplifted Mio-Pliocene mollassic deposits
 - Major depocenter of the SW Alps
- ▶ Mées structure
 - Csup-Eocene basement deformation (Pyrenean orogeny)
 - Possible Alpine reactivation



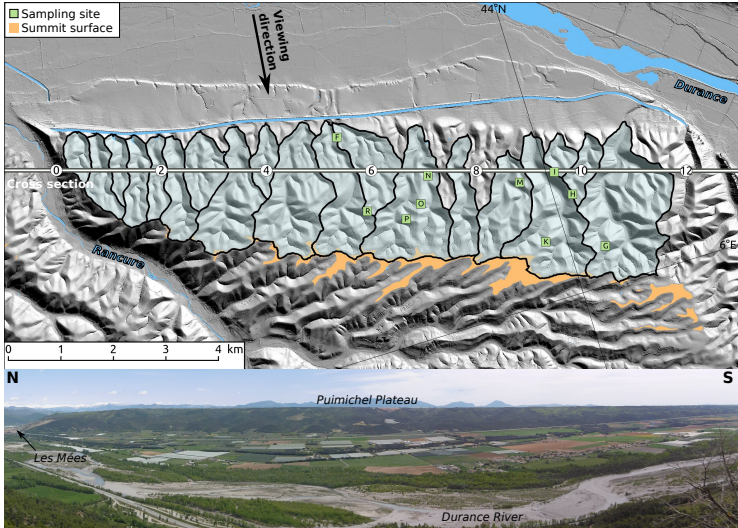
Settings

- ▶ Easily erodible conglomerates
- ▶ Pliocene relict summit surface
- ▶ Major warping of the surface (LiDAR data)



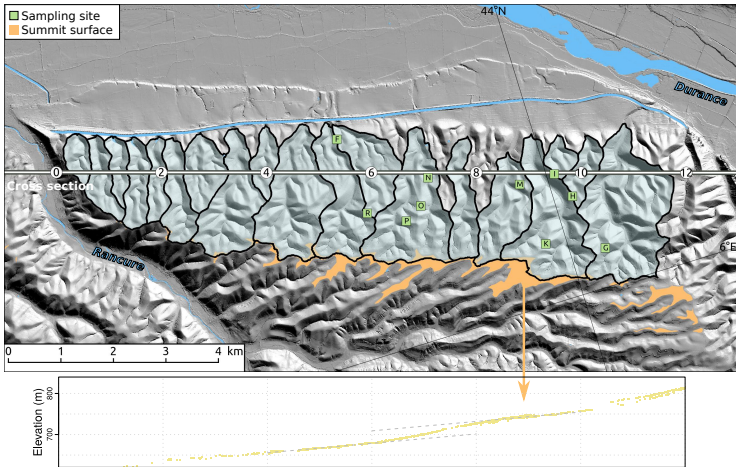
Settings

- ▶ Easily erodible conglomerates
- ▶ Pliocene relict summit surface
- ▶ Major warping of the surface (LiDAR data)



Settings

- ▶ Easily erodible conglomerates
- ▶ Pliocene relict summit surface
- ▶ Major warping of the surface (LiDAR data)



Methods

Hillslope parameters



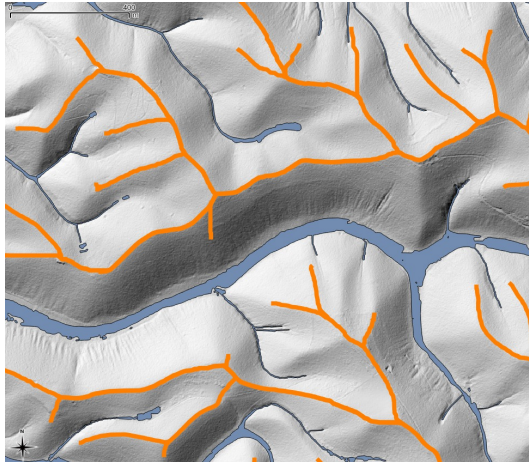
Methods

Hillslope parameters



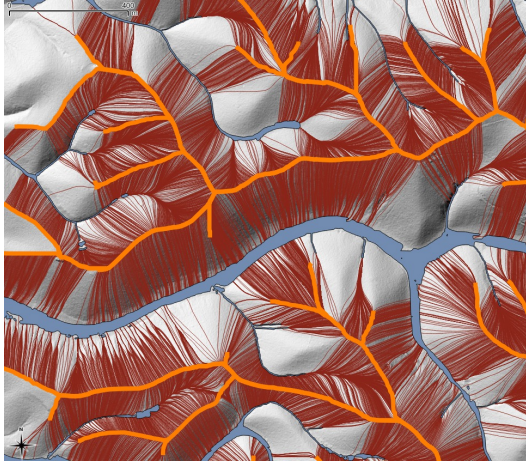
Methods

Hillslope parameters



Methods

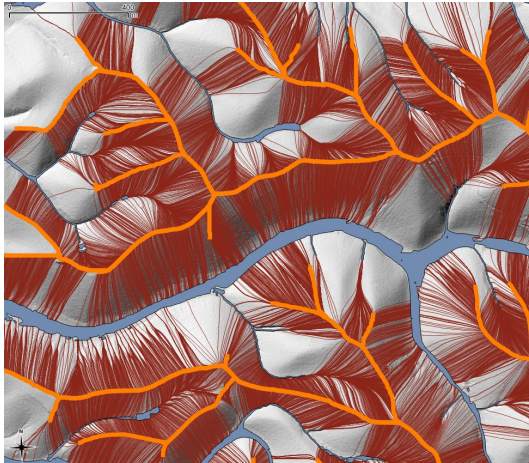
Hillslope parameters



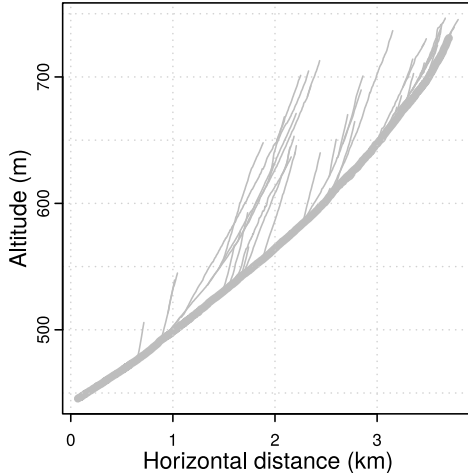
- ▶ Hilltops and flowlines $\Rightarrow R, L_H$ and C_{HT}
- ▶ Hurst *et al.* (2012), Grieve *et al.* (2016),
Clubb *et al.* (2017)

Methods

Hillslope parameters



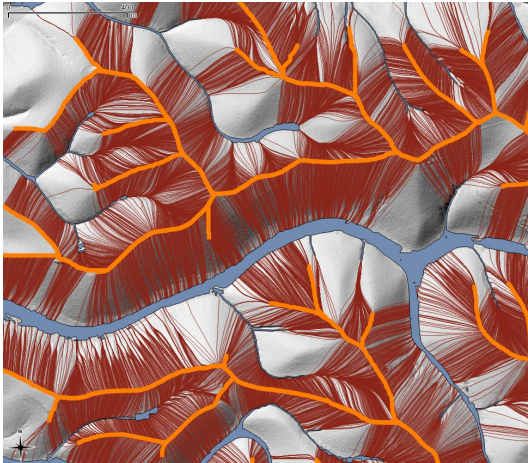
Fluvial parameters



- ▶ Hilltops and flowlines $\Rightarrow R$, L_H and C_{HT}
- ▶ Hurst *et al.* (2012), Grieve *et al.* (2016), Clubb *et al.* (2017)

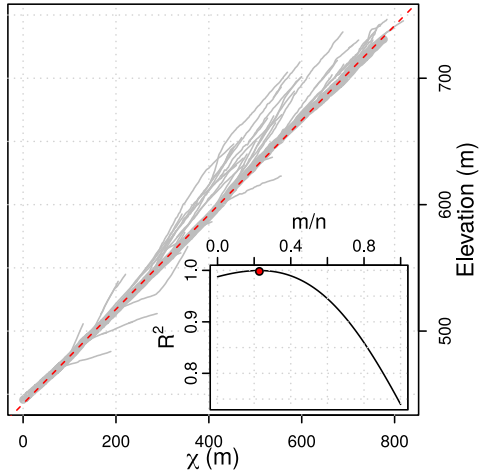
Methods

Hillslope parameters



- ▶ Hilltops and flowlines $\Rightarrow R, L_H$ and C_{HT}
- ▶ Hurst *et al.* (2012), Grieve *et al.* (2016), Clubb *et al.* (2017)

Fluvial parameters

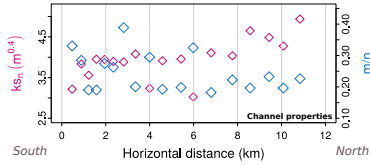


- ▶ Channel profiles $\Rightarrow \theta$ and ks_n ($\theta_{ref} = 0.25$)
- ▶ Perron and Royden (2012)

Results

Spatial distribution of hillslope morphological properties

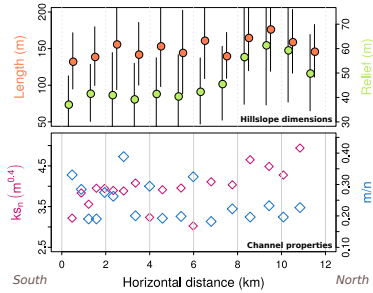
- ▶ A lot of scatter fluvial metrics (slight ks_n increase)



Results

Spatial distribution of hillslope morphological properties

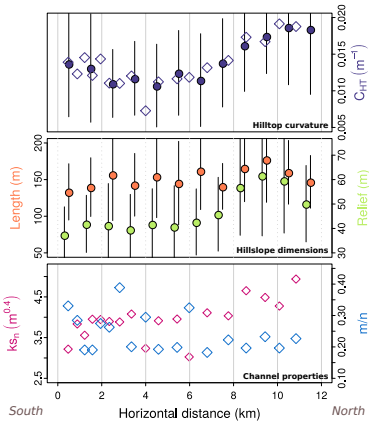
- ▶ Slight increase in relief (R), length (L_H) \sim stable
- ▶ A lot of scatter fluvial metrics (slight ks_n increase)



Results

Spatial distribution of hillslope morphological properties

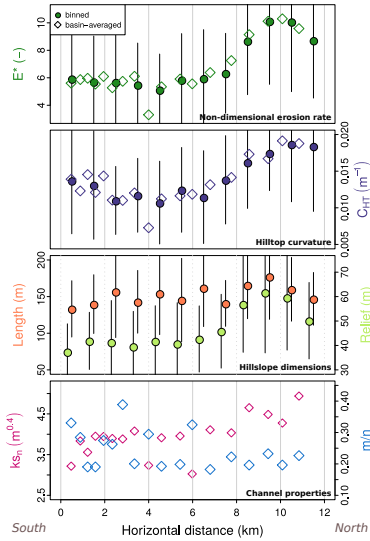
- ▶ 2-fold increase in hilltop curvature (C_{HT})
- ▶ Slight increase in relief (R), length (L_H) \sim stable
- ▶ A lot of scatter fluvial metrics (slight ks_n increase)



Results

Spatial distribution of hillslope morphological properties

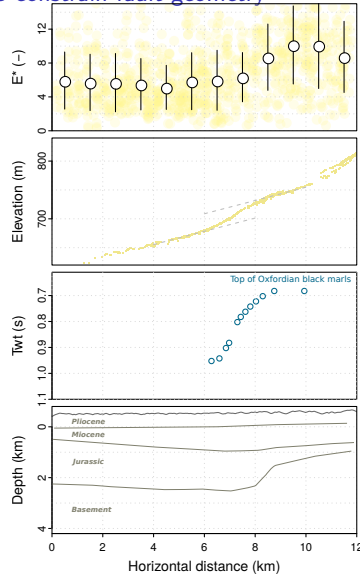
- ▶ Same pattern for E^* ($= 2C_{HT}L_H/S_c$)
- ▶ 2-fold increase in hilltop curvature (C_{HT})
- ▶ Slight increase in relief (R), length (L_H) \sim stable
- ▶ A lot of scatter fluvial metrics (slight ks_n increase)



Results

Inversion of Non-Dimensional Erosion rate (E^*) pattern to constrain fault geometry

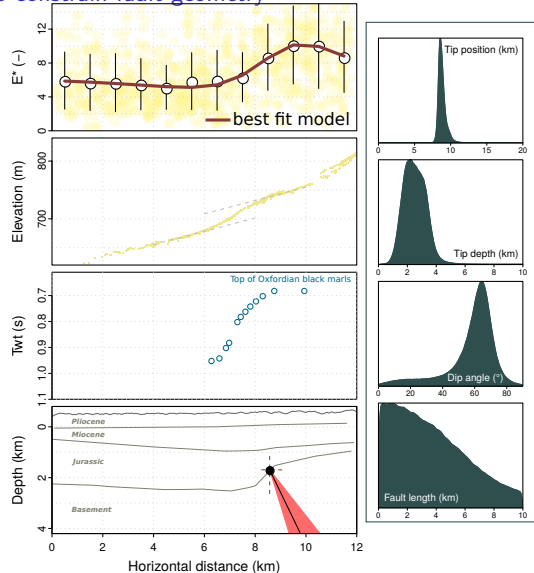
- ▶ Single planar dislocation into a semi-infinite elastic half-space
- ▶ MCMC inversion to retrieve dislocation parameters
 - ▶ Horizontal position
 - ▶ Depth
 - ▶ Dip angle



Results

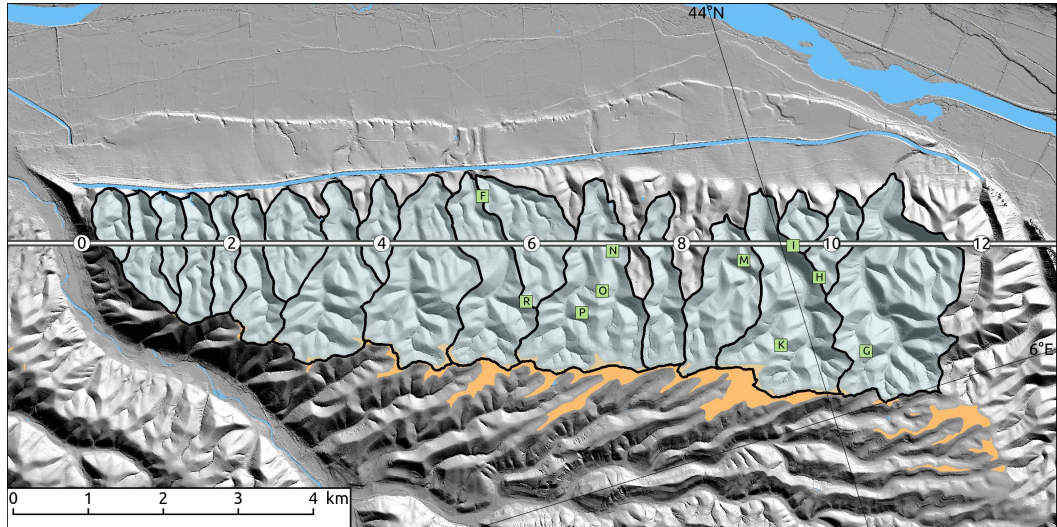
Inversion of Non-Dimensional Erosion rate (E^*) pattern to constrain fault geometry

- ▶ Single planar dislocation into a semi-infinite elastic half-space
- ▶ MCMC inversion to retrieve dislocation parameters
 - ▶ Horizontal position
 - ▶ Depth
 - ▶ Dip angle
- ▶ Globally consistent with available geological data
- ▶ Steep structure reactivated inside the basement
- ▶ Slip rate?



Denudation rates

^{10}Be and ^{26}Al concentrations at hilltop sites



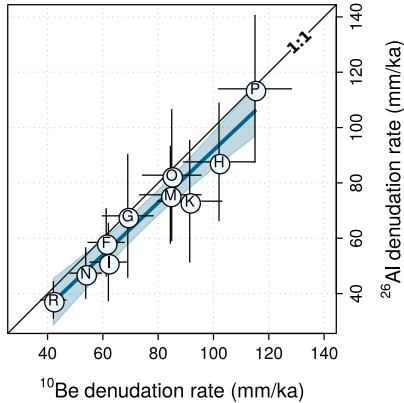
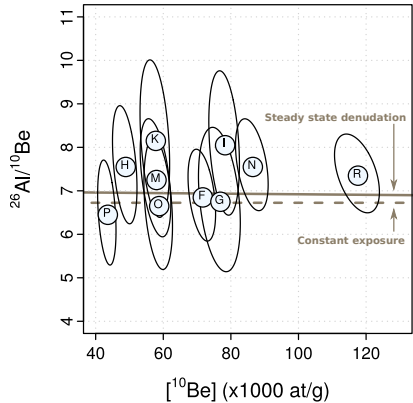
Denudation rates

^{10}Be and ^{26}Al concentrations at hilltop sites



Denudation rates

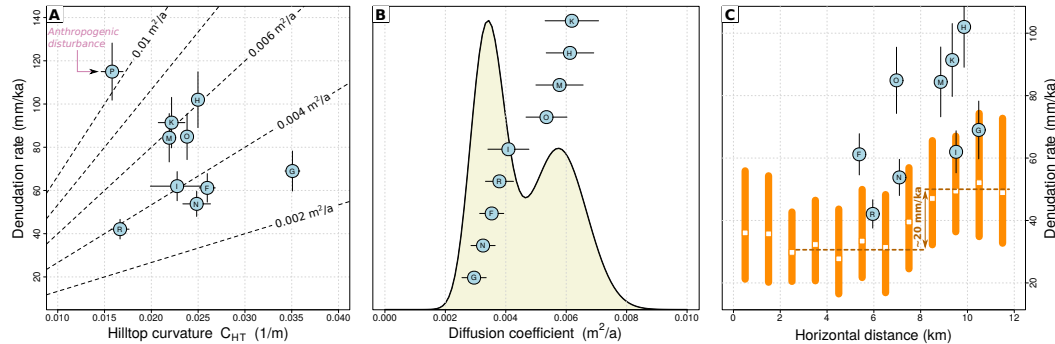
^{10}Be and ^{26}Al concentrations at hilltop sites



- ▶ No apparent inheritance from pre-deposition history
- ▶ Consistent denudation signal from ^{10}Be and ^{26}Al

Denudation rates vs hillslope properties

Converting C_{HT} into denudation rates



- ▶ At shallow slopes near hilltops : $E = \frac{KC_{HT}}{\beta}$
- ▶ ~20 mm/ka differential denudation across the transect
- ▶ Similar amplitude for differential uplift and fault slip rate?

Conclusions

- ▶ HR hillslope morphology analysis allows to decipher denudation and uplift patterns (Hurst *et al.*, 2013, Grieve *et al.*, 2016)
- ▶ High potential in slow deformation areas
- ▶ Higher spatial resolving power than approaches based on river profiles analysis
- ▶ Blind thrust rooted in the basement, folding the Cenozoic cover of the N. Valensole Basin
- ▶ Active thrusting and deformation propagation at the SW Alpine front

